Supporting Information

Enzyme-Responsive Turn-On Nanoprobes for *In Situ* Fluorescence Imaging and Localized Photothermal Treatment of Multidrug-Resistant Bacterial Infections

Xuancheng Du,[a] Weijie Wang,[b] Chun Wu,[d] Bingqing Jia,[c] Weifeng Li,[c] Lin Qiu,[a] Pengju Jiang,[a] Jianhao Wang,[a] and Yong-Qiang Li*[c]*

[a] School of Pharmaceutical Engineering and Life Science, Changzhou University, Changzhou 213164, China.

[b] Shandong Xiandai University, Jinan 250104, China.

[c] Institute of Advanced Interdisciplinary Science, School of Physics, Shandong University, Jinan 250100, China.

[d] State Key Laboratory of Radiation Medicine and Protection, School of Radiation Medicine and Protection, Collaborative Innovation Center of Radiological Medicine of Jiangsu Higher Education Institutions, Soochow University, Suzhou 215123, China.

Experimental

Photothermal effects of AuNS-Apt-Cy nanoprobes

To assess the photothermal effect of our nanoprobe, 0.5 mL of AuNS-Apt-Cy water solutions with different concentrations (0.1, 0.2, 0.4, 0.5 nM) were irradiated using a NIR laser (808 nm, 0.5 W/cm^2) for 5 min during which the sample temperature was continually monitored by a thermal imager, and about 600 temperature data at different irradiation times were obtained in 300 s irradiation. By using line to connect the temperature data points at 1, 2, 3, 4, and 5 min in the software of Origin, photothermal heating curves of AuNS-Apt-Cy nanoprobes could be plotted.

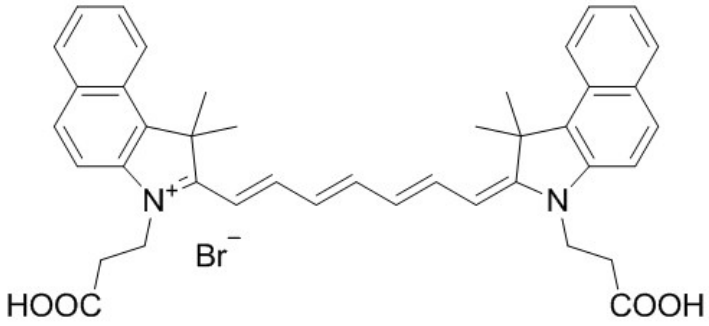

Figure S1. The molecular structure of Cypate dye.

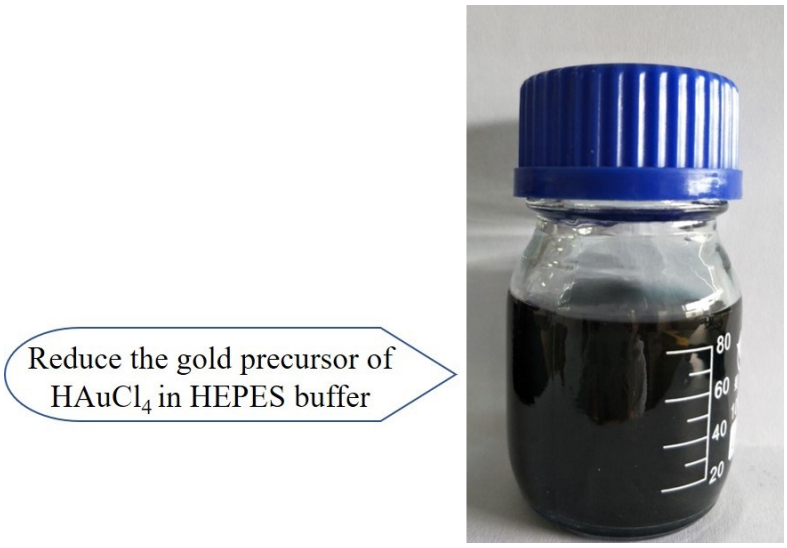

Figure S2. Large-scale synthesis of AuNS based on the reduction of gold precursor of $HAuCl_4$ in HEPES buffer, where the HEPES acts as both the reducing and shape-directing agent.

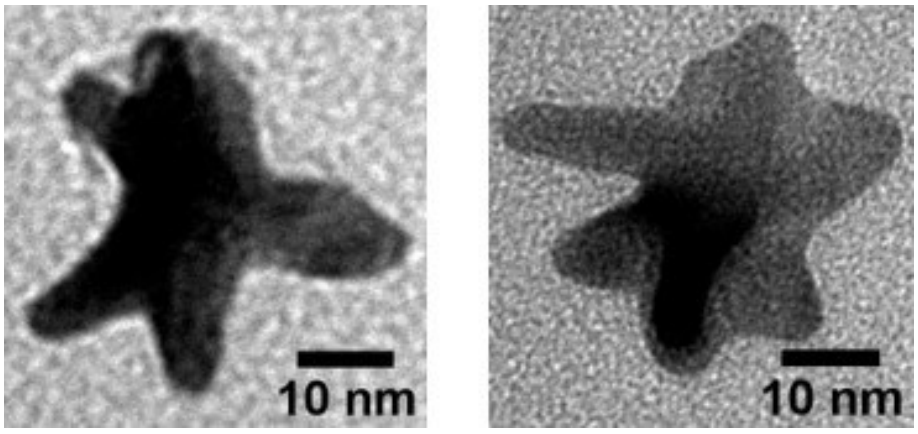

Figure S3. TEM images of AuNS-Apt-Cy nanoprobe with multiple spikes.

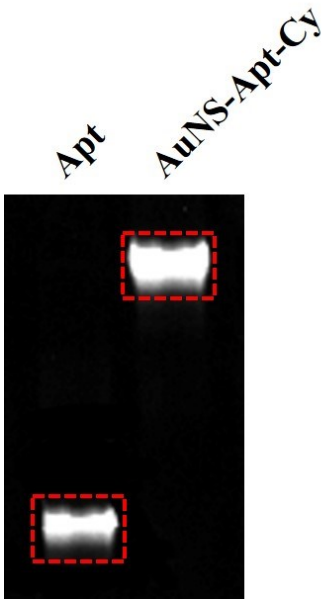

Figure S4. Agarose gel electrophoresis of Apt and AuNS-Apt-Cy nanoprobe.

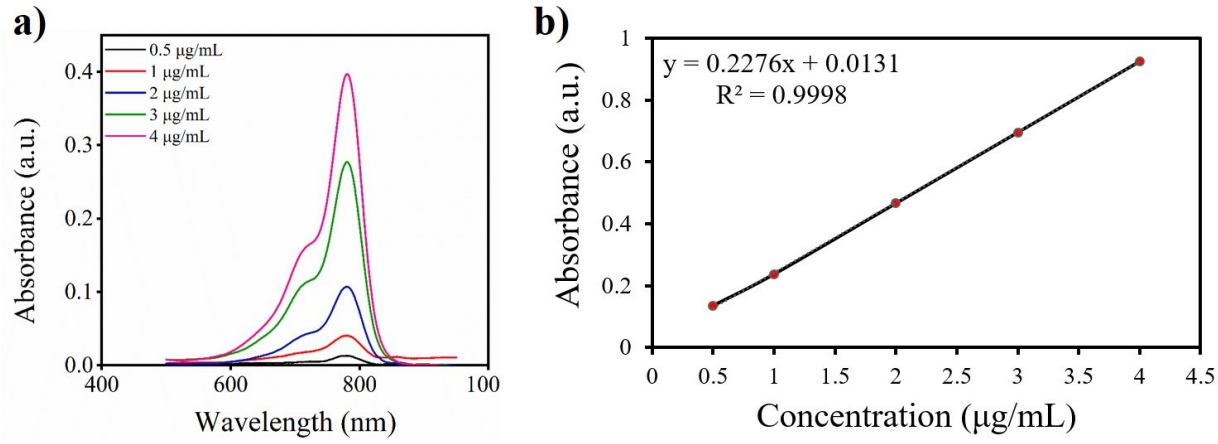

Figure S5. a) Absorbance spectra of cypate with various concentrations ranged from 0.5 to 4 µg/mL. b) The linear calibration curve between cypate concentration and its absorbance.

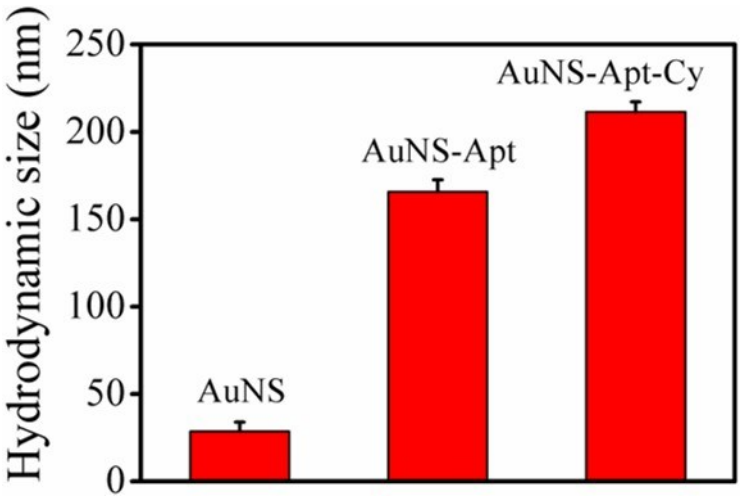

Figure S6. Hydrodynamic size of AuNS, AuNS-Apt, and AuNS-Apt-Cy in PBS buffer.

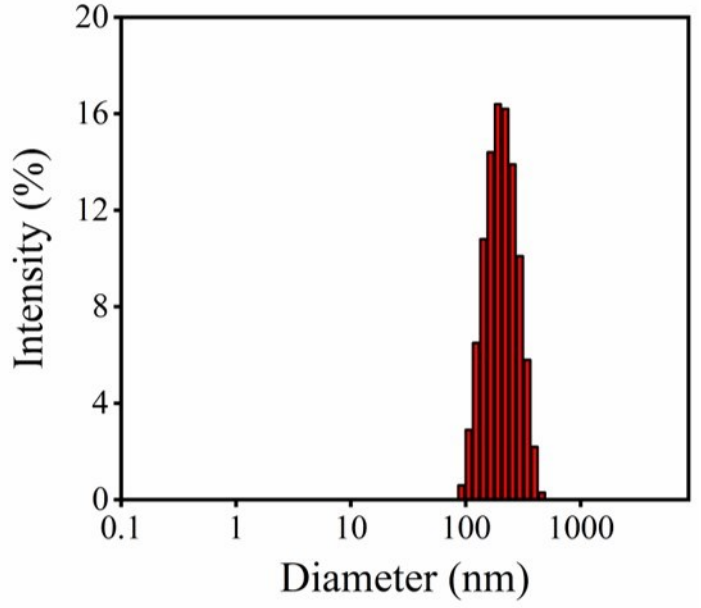

Figure S7. Hydrodynamic size of AuNS-Apt-Cy nanoprobe in PBS buffer.

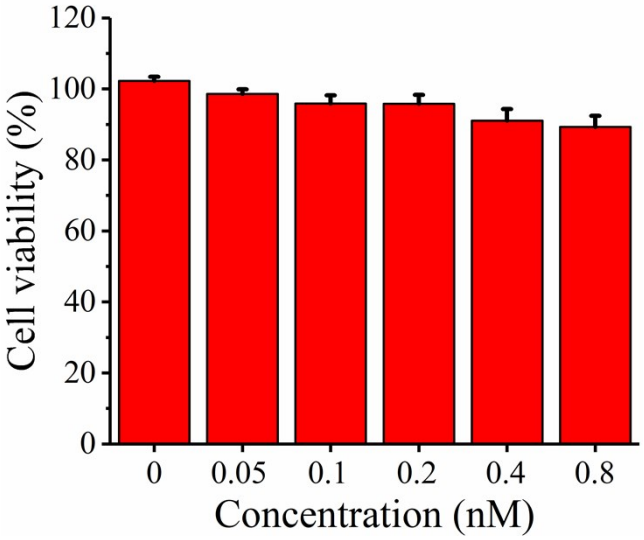

Figure S8. Viability of NIH-3T3 cells after incubation with different concentrations (0, 0.05, 0.1, 0.2, 0.4, 0.8 nM) of AuNS-Apt-Cy nanoprobes for 1 day. In this experiment, AuNS-Apt-Cy and AuNS-Cy modified with increased concentration of HS-PEG molecules (from 1.64 mg/mL to 5 mg/mL) during their preparation were employed.

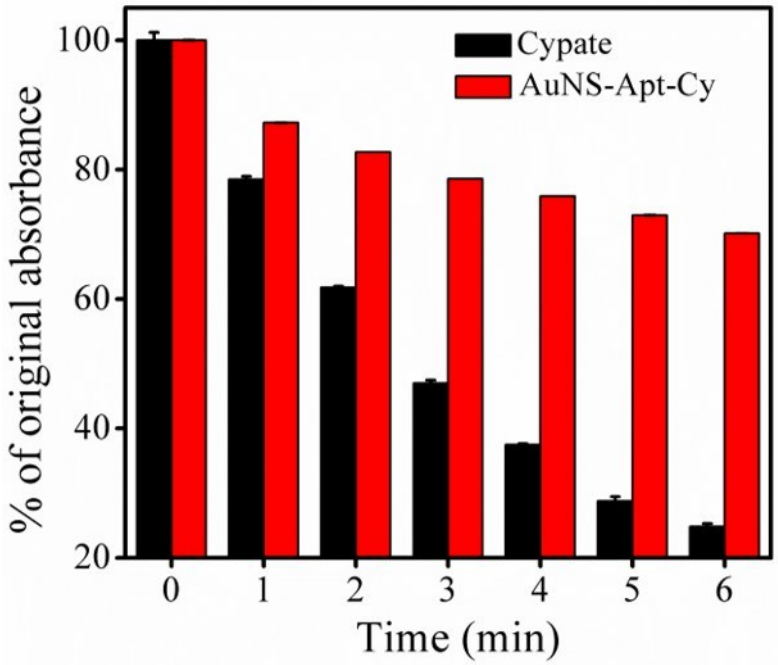

Figure S9. The decay histograms of Cypate and AuNS-Apt-Cy upon NIR laser (808 nm, 0.5 W/cm^2) irradiation for 5 min based on the absorption spectroscopic monitoring.

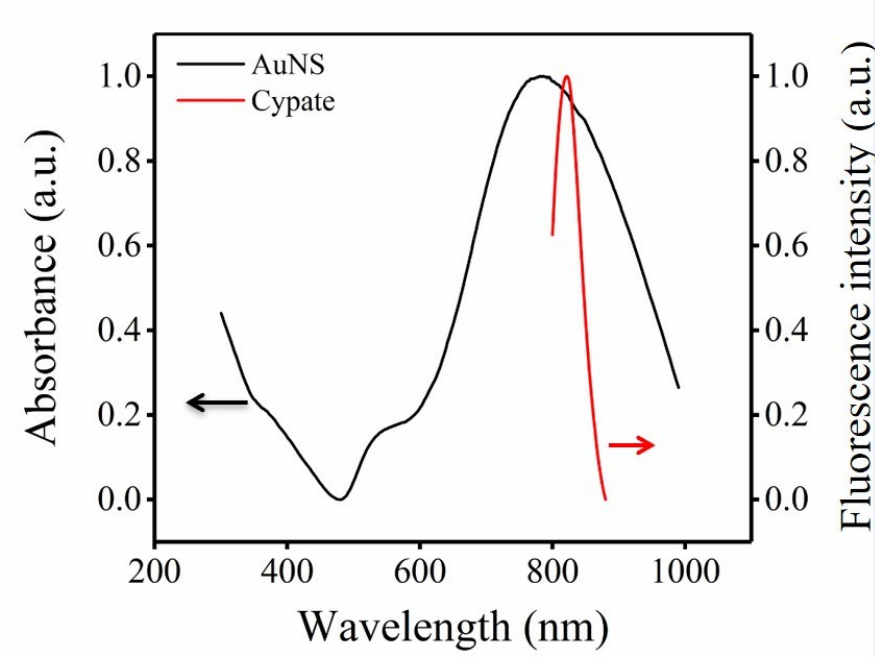

Figure S10. Absorption spectrum of AuNS and fluorescence emission spectra of cypate dye.

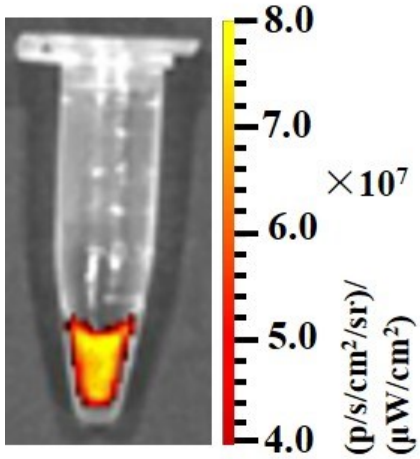

Figure S11. *In vitro* NIR fluorescence imaging of AuNS-Apt-Cy nanoprobes (0.4 nM) after incubation with MRSA culture supernatant for 30 min. MRSA culture supernatant was obtained by centrifuging the MRSA culture to remove the MRSA bacterial cells inside.

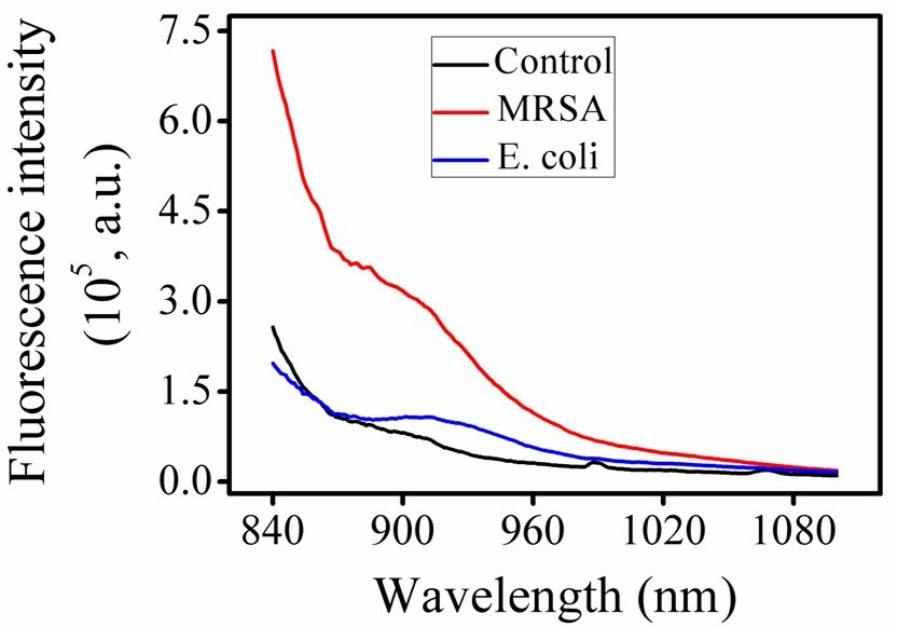

Figure S12. Fluorescence spectra of AuNS-Apt-Cy (0.4 nM) before (control) and after incubation with different bacterial cultures (MRSA or *E. coli*) for 30 min.

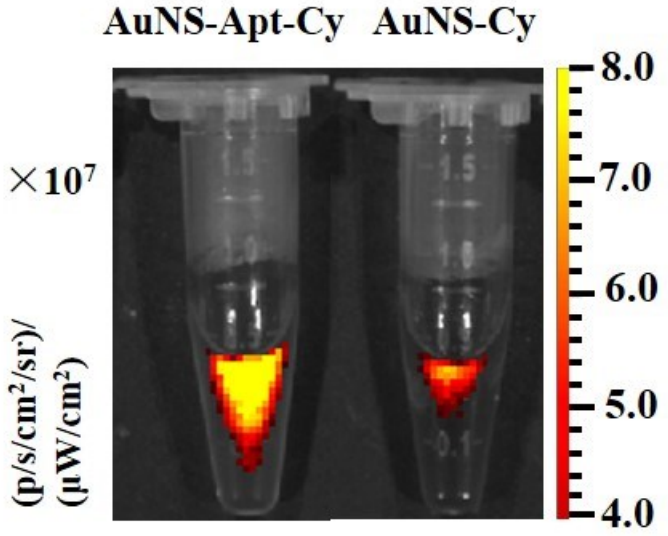

Figure S13. *In vitro* NIR fluorescence imaging of AuNS-Apt-Cy and AuNS-Cy with the same concentration (0.4 nM) after incubation with MRSA (2×10^5 CFU) for 30 min. In this experiment, AuNS-Apt-Cy and AuNS-Cy modified with increased concentration of HS-PEG molecules (from 1.64 mg/mL to 5 mg/mL) during their preparation were employed.

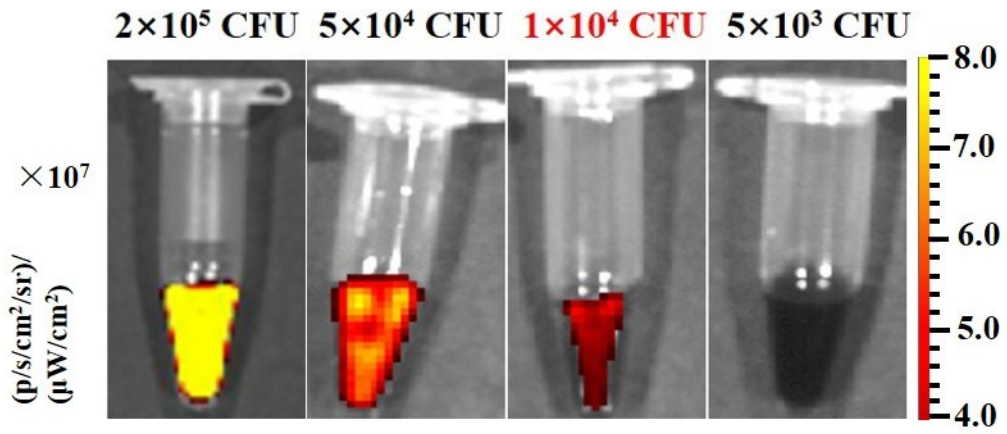

Figure S14. *In vitro* NIR fluorescence imaging of AuNS-Apt-Cy after incubation with different concentrations of MRSA for 30 min.

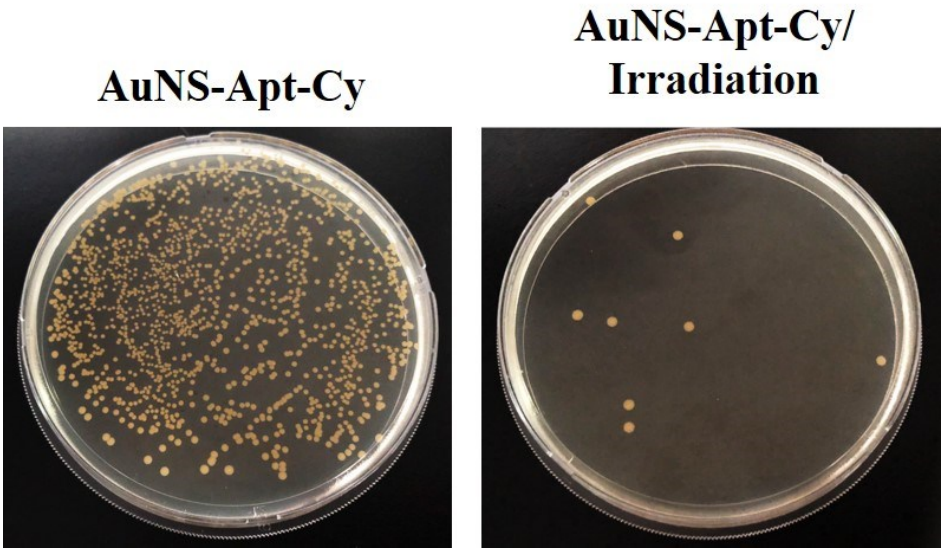

Figure S15. Photographs of MRSA cultures (10^6 CFU/mL) incubated with AuNS-Apt-Cy (0.4 nM) before and after NIR laser irradiation (808 nm, 0.5 W/cm^2, 5 min).

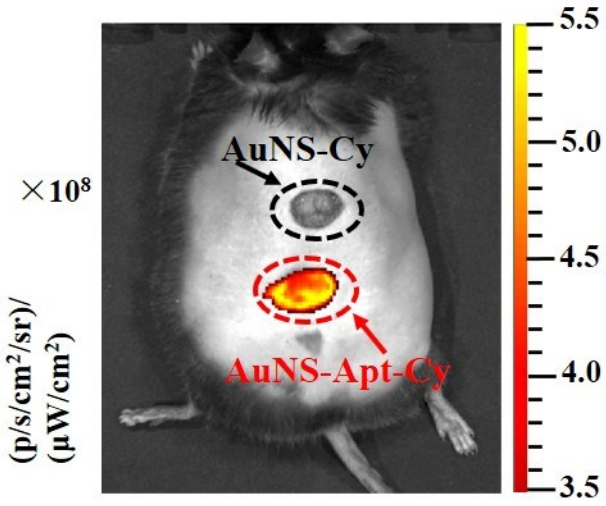

Figure S16. *In situ* NIR fluorescence imaging of diabetic mouse with MRSA-infected wound at 1 h post-spraying of AuNS-Apt-Cy and AuNS-Cy with the same concentration (0.8 nM). In this experiment, AuNS-Apt-Cy and AuNS-Cy modified with increased concentration of HS-PEG molecules (from 1.64 mg/mL to 5 mg/mL) during their preparation were employed.

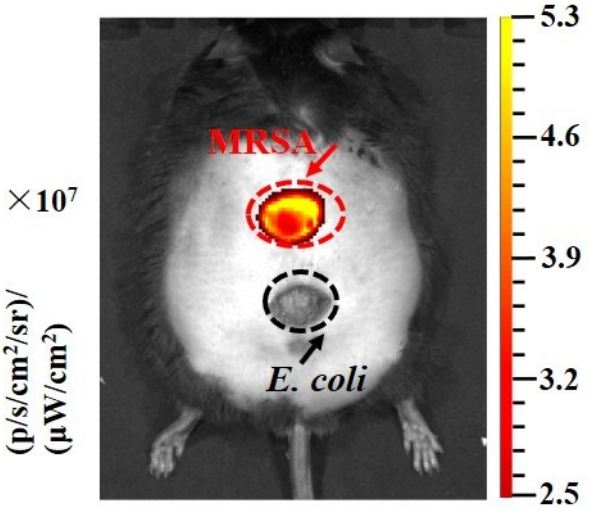

Figure S17. *In situ* NIR fluorescence imaging of diabetic mouse with MRSA and *E. coli*-infected wound at 1 h post-injection of AuNS-Apt-Cy (0.8 nM). In this experiment, AuNS-Apt-Cy modified with increased concentration of HS-PEG molecules (from 1.64 mg/mL to 5 mg/mL) during their preparation were employed. The AuNS-Apt-Cy nanoprobes were intravenously injected into the infected mice through the tail vein.

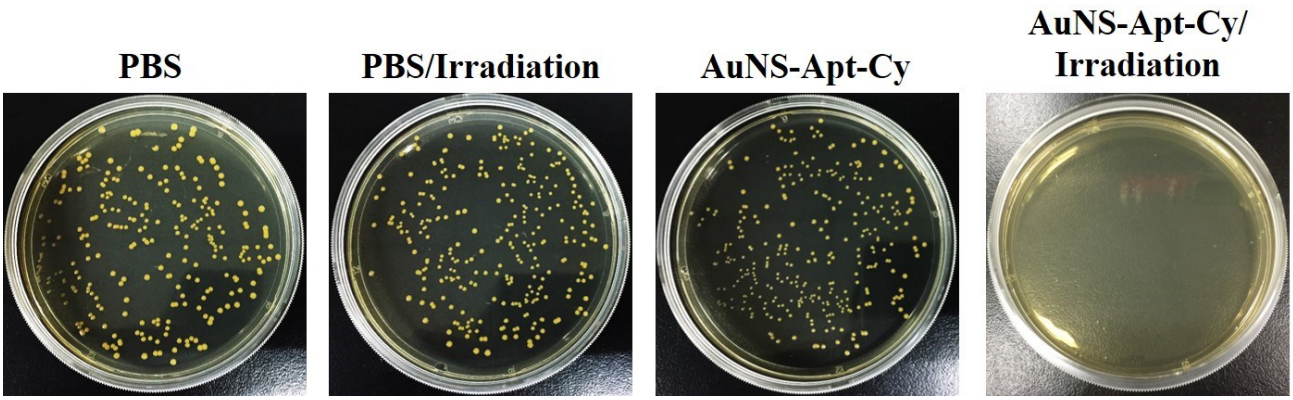

Figure S18. Photographs of bacterial cultures from the skin tissues of MRSA-infected diabetic wound in four treatment groups (PBS, PBS/irradiation, AuNS-Apt-Cy, AuNS-Apt-Cy /Irradiation). NIR laser irradiation (808 nm, 0.5 W/cm^2, 5 min) was employed.

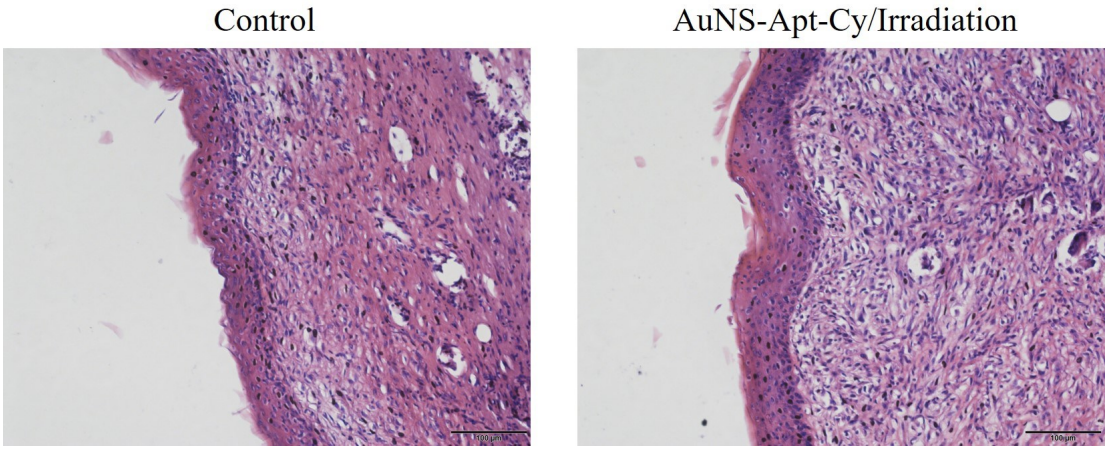

Figure S19. Representative H&E staining images of the skin tissue surrounding the MRSA-infected wound of diabetic mouse on the 8th day treatment of AuNS-Apt-Cy/Irradiation. The normal skin tissue of diabetic mouse was used as the control, and NIR laser irradiation (808 nm, 0.5 W/cm^2, 5 min) was employed.

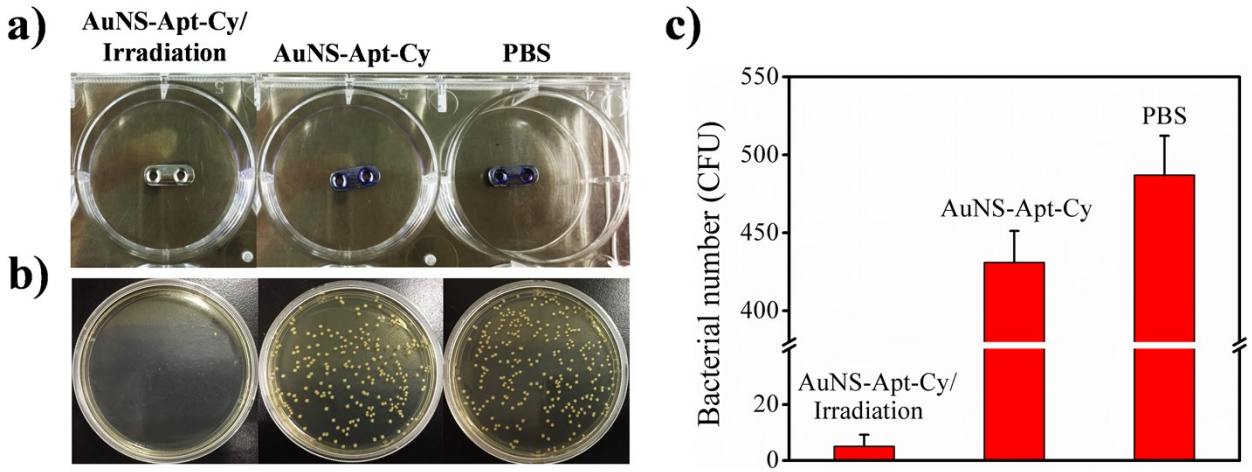

Figure S20. a) Representative photographs of implanted bone plates taken from the subcutaneous tissue of mice after different treatment. b) Representative photographs of bacterial cultures from the implanted bone plates taken from the subcutaneous tissue of mice after different treatment. c) Corresponding MRSA colony numbers counted based on the culture images shown in (b). The values of bacterial number represent the mean of three independent experiments, and the error bars indicate the SD from the mean.

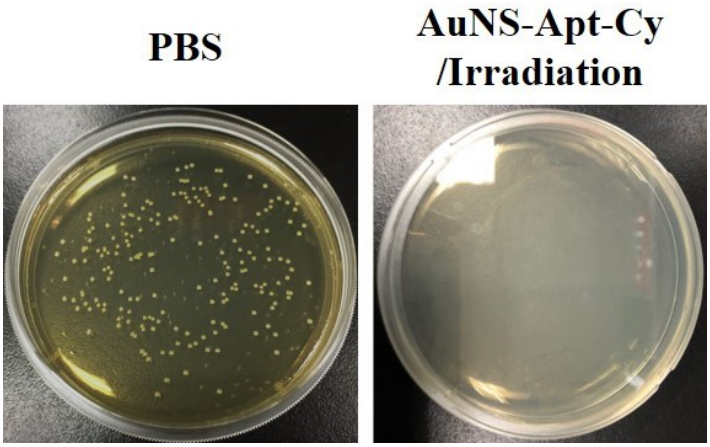

Figure S21. Representative photographs of bacterial cultures from the implanted bone plates taken from the subcutaneous tissue of mice after different treatment. In the treatment group of AuNS-Apt-Cy/Irradiation, the infected site was first irradiated with an NIR laser (808 nm, 0.5 W/cm^2) for 5 min and the implanted MRSA-infected bone plate was then taken out at 1 h post-injection of AuNS-Apt-Cy.

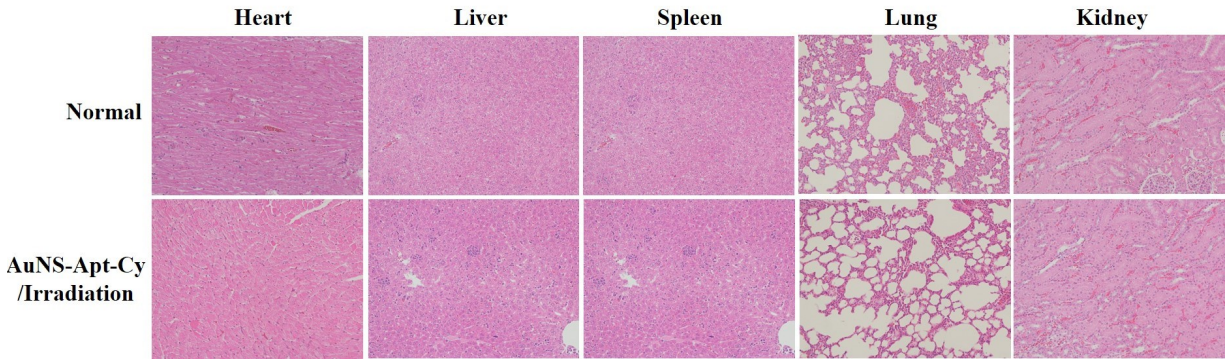

Figure S22. The H&E staining images of different organs of mice implanted with MRSA-infected bone plate on the 2nd day treatment of AuNS-Apt-Cy/Irradiation. NIR laser irradiation (808 nm, 0.5 W/cm^2, 5 min) was employed.

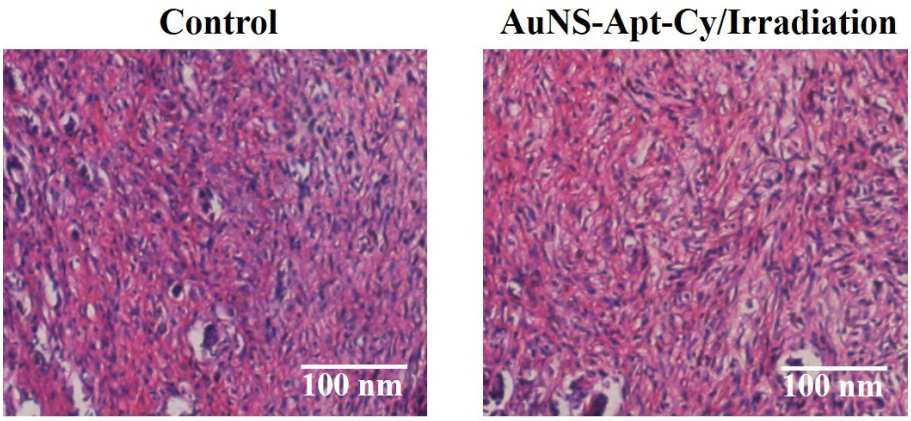

Figure S23. Representative H&E staining images of subcutaneous tissue surrounding the MRSA-infected implanted bone plate of mouse on the 2nd day treatment of AuNS-Apt-Cy/Irradiation. The normal subcutaneous tissue of mouse was used as the control, and NIR laser irradiation (808 nm, 0.5 W/cm^2, 5 min) was employed.